University of Huddersfield Repository

Abdulwahab, Abubaker and Mishra, Rakesh

Estimation of LTR rollover index for a high-sided tractor semitrailer vehicle under extreme crosswind conditions through dynamic simulation

Original Citation

Abdulwahab, Abubaker and Mishra, Rakesh (2017) Estimation of LTR rollover index for a high-sided tractor semitrailer vehicle under extreme crosswind conditions through dynamic simulation. In: 23rd International Conference on Automation and Computing (ICAC 2017). IEEE. ISBN 978-0-7017-0260-1

This version is available at http://eprints.hud.ac.uk/id/eprint/33343/

http://eprints.hud.ac.uk/

Estimation of LTR rollover index for a high-sided tractor semitrailer vehicle under extreme crosswind conditions through dynamic simulation

Abubaker Abdulwahab
School of Computing & Engineering
University of Huddersfield
Huddersfield, UK
Abubaker.Abdulwahab@hud.ac.uk

Rakesh Mishra
School of Computing & Engineering
University of Huddersfield
Huddersfield, UK
r.mishra@hud.ac.uk

Abstract— **Lateral load transfer ratio (LTR) is a criterion that is often used for designing ground vehicle rollover warning technologies to indicate the vehicles rollover status. Generally, LTR index depends on road geometry and vehicle characteristics. However, crosswind loads have the potential to influence the roll stability and therefore the safety of road vehicles particularly large commercial units. This study provides improved methodology for the computation of the LTR index for a high-sided tractor semitrailer vehicle under crosswind conditions. For this purpose, since experiments on real vehicles for active safety technology are difficult to carry out, a coupled simulation of transient crosswind aerodynamics and multi-body vehicle dynamics has been proposed. Based on CFD method, a large-eddy simulation (LES) technique was employed to predict the transient crosswind aerodynamic forces. Then, the predicted aerodynamic forces were input into multi-body dynamic simulations of the tractor semi-trailer vehicle that were performed through ADAMS/Car software. Simulation results show that comparing to the traditional LTR index, the LTR under crosswind is more efficient to detect manoeuvre-induced rollovers. This trailer rollover indicator that has been improved by the proposed methodology can provide more reliable information to the warning or control system in the presence of wind conditions.**

Keywords— *Dynamic Simulation; Rollover; Crosswind; Multibody; CFD*

I. INTRODUCTION

The safety of large class vehicles is a common concern for all roads users. Compared to other types of ground vehicles, commercial vehicles like a high-sided tractor semitrailer unit usually have large body with a high center of gravity and considerable loading capacity. As a result of this design, these vehicles are known to be at higher risk of overturning accidents. Due to various reasons, rollover may not be effectively detected by vehicle control systems, or drivers may be unaware of the upcoming rollover specially for heavy vehicles [1]. Thus, it is vital to develop an effective active or a passive rollover detection system (e.g. roll stability control) for facilitating early prevention to avoid vehicle-rollover accidents.

Development of a predictor for the likelihood of a vehicle rollover is an important challenge in the development of active/passive rollover control systems[1]. A number of rollover metrics have been introduced by various researchers[2][3][4]. A Static stability factor (SSF) is one such predictor that has been proposed by NHTSA to detect vehicle rollover condition[2]. It is a basic rollover criteria, which is defined as the ratio between half of the wheel track width and the CG height. The system warns of an imminent rollover of the vehicle, when the lateral acceleration exceeds the SSF value. However, in dynamic situations, the SSF by itself is not a useful and reliable indicator [4]. In [3] a lateral Load Transfer Ratio (LTR) has been suggested for use in a rollover control system. The LTR index is the relation of difference between the right vertical tire force and the left vertical tire force of a vehicle axle divided by the vehicle's total weight. The LTR indicator can vary from 0 when the normal force on a vehicle wheels of both sides are equal, to 1 when the wheels lift off. However, the author stated that there is no simple method exists for directly measuring the normal wheel loads. In order to solve this problem, several studies [1][4-7] have been conducted to obtain implementable version of the LTR index. Reference [7] developed algorithms to estimate state and parameters of a vehicle for reliable computation of the LTR index. The investigated algorithms include a sensor fusion algorithm that utilizes a low-frequency tilt angle sensor and a gyroscope, and a nonlinear dynamic observer that utilizes only a lateral accelerometer and a gyroscope. In [5] another solution was proposed: a predictive model to determine a rollover threat index associated with tractor-semitrailers combination. They used the LTR coefficient in which, several key parameters were obtained using system identification techniques.

It can be seen from the above discussion that parameters of the rollover reported in literature depend either on vehicle states or on road geometry factors. However, there has been limited investigation into other factors affecting vehicle rollover index such as strong crosswind forces[8]. Crosswind effects become critical when the vertical load on one or more wheels is already low due to the other effects described here. In addition, according to references [9][10], high-sided commercial vehicles are particularly sensitive to the unsteady

crosswind conditions when running on exposed sites where topographical features of the landscape magnify the wind effects. In the reported studies, vehicle aerodynamic information was employed to find accident speeds for ground vehicles under a strong crosswind. It has been also reported that the crosswind aerodynamic forces such as drag, lift and side forces induce different dynamic responses to the ground vehicles, and directly impact the lateral acceleration and roll motion.

In general, there are two approaches to predict aerodynamic characteristics of ground vehicles under crosswind conditions, one is to use experimental tools such as scale-model wind-tunnel testing, or perform on-road measurements. The second approach is to simulate numerically the wind flow over the vehicle by using computational fluid dynamics (CFD) techniques [11]. CFD can provide a large amount of transient data and detailed three-dimensional information about the flow field.

This study introduces improved LTR rollover index to effectively detect effects of crosswind forces on a vehicle rollover. A high-sided tractor semitrailer unit is considered, and a coupled analysis of unsteady aerodynamics and multi-body dynamics have been applied to the combination. Firstly, the vehicle aerodynamics effects in transient crosswind were obtained numerically by using a Large-Eddy Simulation (LES) method for modeling wind turbulence. Then, components of predicted aerodynamic forces acting on the truck were input into the vehicle multi-body dynamic system. Finally, the simulation data of a constant radius turning maneuvers conducted by the ADAMS/Car software was employed to calculate the LTR for the trailer axles.

II. VEHICLE AERODYNAMICS SIMULATION

This section presents a summary of the Large-Eddy Simulations (LES) that was carried out to predict unsteady vehicle aerodynamic forces. The Navier-stokes equations are solved numerically using the ANSYS-FLUENT 17.0.0 solver. An incompressible Newtonian fluid was assumed, and the time-dependent Navier-Stokes equations were spatially filtered to acquire the governing equations of the LES as follows

$$\frac{\partial \bar{u}_i}{\partial x_i} = 0$$

$$\frac{\partial (\rho \bar{u}_i)}{\partial t} + \frac{\partial (\rho \bar{u}_i \bar{u}_j)}{\partial x_j} = -\frac{\partial \bar{P}}{\partial x_i} + \frac{\partial}{\partial x_j}\left(\mu_t \frac{\partial \bar{u}_i}{\partial x_j}\right) - \frac{\partial \tau_{ij}}{\partial x_j} \quad (1)$$

$$\mu_t = \rho L^2 |\bar{S}| \quad (2)$$

$$\tau_{ij} = -2\mu_t \bar{S}_{ij} + \frac{1}{3}\tau_{kk}d_{ij} \quad (3)$$

where $\bar{u}$ being the filtered velocity vector, $\bar{P}$ is the filtered pressure field, τ is sub-grid-scale stresses and ρ, ν are the fluid density and kinematic viscosity, respectively. $\bar{S}$ is the filtered rate of strain tensor, which given as:

$$\bar{S}_{ij} \equiv 0.5 \left(\frac{\partial \bar{u}_j}{\partial x_i} + \frac{\partial \bar{u}_i}{\partial x_j}\right) \quad (4)$$

L is the mixing length of sub-grid-scales; $L = min[\kappa d, C_s^{LES}, \Delta]$, with $\kappa = 0.41$ being the von Karman constant, d is the distance to the closest wall, and $C_s^{LES}=0:1$ [19]. $\Delta = \Delta_x \Delta_y \Delta_z$ with Δi being the local computational cell size in the i-Cartesian coordinate. For further information on the characteristics of the LES technique see reference [12] .

A. Numerical set-up and boundary conditions

The numerical simulation of a realistic atmospheric wind as similar as possible to the crosswind wind experienced by the tractor semitrailer was carried out by using the spectral synthesizer algorithms [13].This algorithm is available in ANSYS_FLUENT package to model the fluctuating velocity at velocity inlet boundaries. The approach is based on a random flow generation technique, originally proposed by [14] and modified in [15].

As shown in Figure (1), the conventional computational domain (box shape) has been created around the vehicle model to simulate the crosswind conditions. The domain with a 124.5 m length, 126.0 m width, and 32.0 m height was used to capture the essential flow features[16]. Tetrahedral unstructured meshing scheme was used to discretize the computational fluid domain into about 27.6 million finite volumes. The number of elements has been chosen after several mesh configurations were tested to check the grid independency. Furthermore, the maximum skewness of the meshed geometry was 0.79, and the topology of these meshes is illustrated in Figure 1- (b). In the figure, two refinement zones are shown, the finest cells zone and the upstream zone; the fine cells are created to capture the small flow structures around the vehicle.
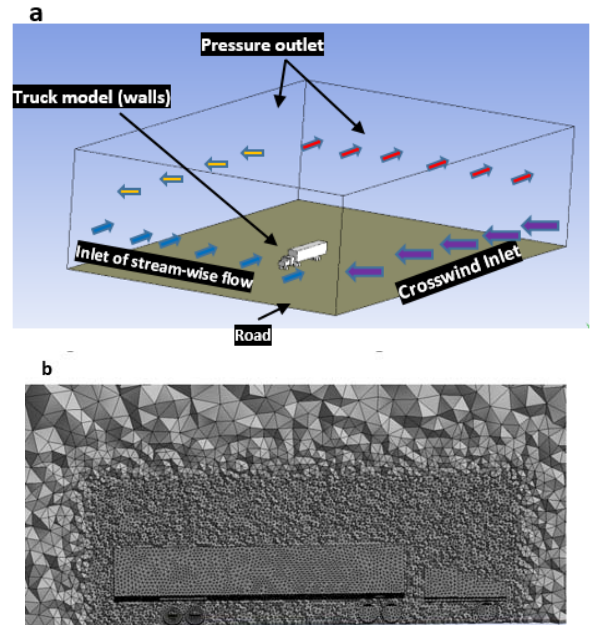

Figure 1 : (a) computational domain (b) mesh topology

The vehicle model used in the present calculations is a full-scale model of a tractor semi-trailer unit and was built in ADAMS/Car software version 2015.1.1. The model is based on geometry of a real commercial vehicle. It has been chosen to predict accurately vehicle dynamic responses to wind actions through ADAMS simulation [17]. The 3-D model is shown in Figure 2. The trailer's axles are adapted slightly by eliminating small parts attached to their surface because of their negligible effect. The geometry length L, width B, and height H used are 20.86 m, 2.6m, and 4.16m, respectively. The vehicle is anticipated to move directly ahead at a continuous speed of 30 m/s, which is the speed limit for heavy vehicle according to legislations [16]. To simulate the vehicle movement, no-slip condition is used at the fixed trailer surface and the road, while velocity of 30 m/sec is applied at inlet of stream-wise flow.

Furthermore, in order to reproduce a strong crosswind across the pathway of the trailer, a fluctuating crosswind with mean velocity of 30 m/sec was imposed on the side boundary of the domain as second flow inlet[18]. A symmetry boundary condition (i.e. zero normal velocity) is assigned to the top boundary, and the uniform atmosphere pressure is imposed at the main and lateral outlet walls of the domain. The SIMPLE method is used for solving the pressure–velocity coupling, the spatial discretization schemes used are second order for the pressure equation and bounded central difference for the momentum equation. Abounded second order implicit scheme is chosen for the transient terms. A constant time step of $\Delta t = 12 \times 10^{-4}$ s was used to achieve the Courant-Friederich-Lewy (CFL) number below 1. Wind loads on the vehicle are commonly calculated by means of aerodynamic coefficients as follows[19]:

$$F_{D,S,L}(t) = \frac{1}{2} \rho_{air} A\ C_{(D,S,L)}\ v_{rel}^2(t) \qquad (5)$$

where ρ_{air} is the air density, A is a reference area and h is a reference height. $F_{D,S,L}(t)$ are aerodynamic forces for drag F_D, lift F_L and side force F_S, and the corresponding aerodynamic coefficients are C_D, C_L and C_S. The vehicle speed relative to the wind can be defined directly as a function of the absolute wind speed time-history u(t) seen by a vehicle of V_{tr} speed, and it is defined as:

$$v_{rel}^2(t) = (V_{tr} + u(t) \cos \alpha)^2 + (u(t) \sin \alpha)^2 \qquad (6)$$

where α is the wind angle relative to the vehicle's travel direction. In these computations, the time-series of crosswind velocity u(t) was sampled at a point just opposite to the trailer's aerodynamic center (wind pressure center) (Figure 2) where the most critical conditions occur [11]. The determination of the pressure center location was based on option available in the ANSYS fluent solver, and it is observed
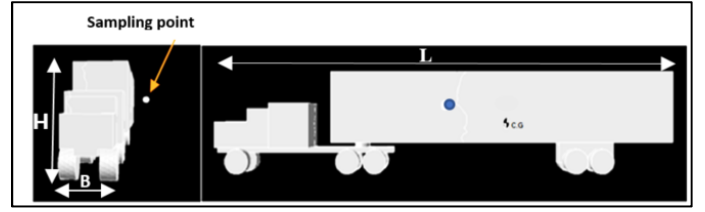

Figure 2 : Vehicle geometry and sampling point

that this location is almost unchanged under wind fluctuation effects.

The fluctuation of the wind velocity profile at sampling point is plotted in the Figure 3. Furthermore, Figure 4 presents time history of the trailer aerodynamic forces. As it can be seen from the figure, the forces increase and decrease corresponding to the crosswind velocity magnitude up to 8 second of motion, after which fluctuations diminish. The figure also shows that the unsteady wind effects are significant on lateral and lift aerodynamic forces as compared to the drag force.
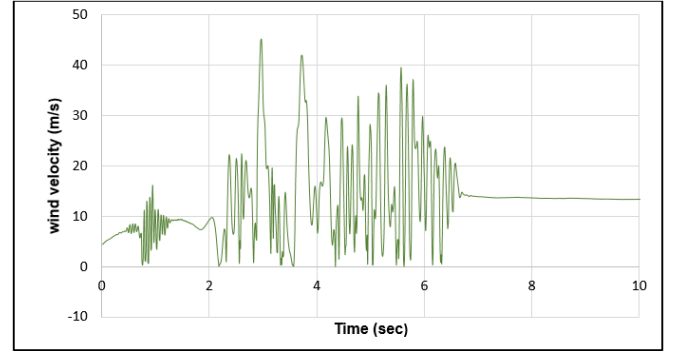

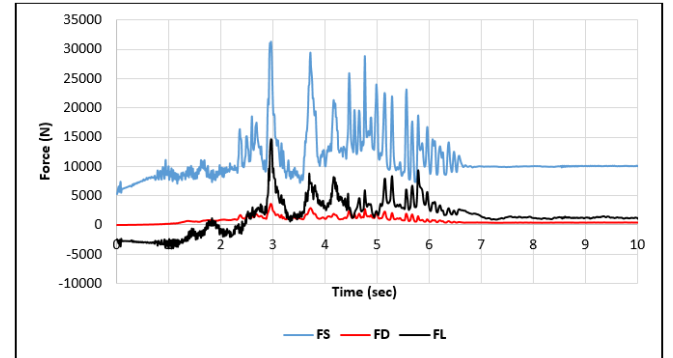Figure 3 : CFD crosswind velocity profile

Figure 4 : unsteady crosswind aerodynamics forces

III. ROLLOVER DYNAMICS OF THE TRACTOR SEMITRAILER COMBINATION

Mathematical models of tractor-semitrailer dynamics are a very complex [20], so as mentioned previously ADAMS/Car software is employed to evaluate the vehicle roll dynamics under crosswind conditions. The prototype of tractor semitrailer unit consists of two main parts, first part is the tractor and second part is the trailer. The tractor model was divided into nine subsystems which consist of steering system,

brake system, front suspension, rear suspension, front wheel and tire, powertrain, tractor body and the fifth wheel. The trailer model was divided into seven subsystems: trailer body, rear and front independent suspension of the trailer. Attached to the suspension subsystem is the subsystem representing rear and front tires.

ADAMS solver allows the user to write customized FORTRAN/C++ routines or to import experimental/numerical data to incorporate forces, constraints, and motions that are not included in the ADAMS libraries. This is particularly useful in this work because it allows the incorporation of aerodynamic forces into the vehicle dynamics model. Therefore, time-dependent splines tool was used to incorporate the tractor semitrailer aerodynamic forces into the ADAMS model. As shown in Figure 5, the aerodynamic loads that were computed in the previous section were applied to the system using a VFORCE element which located at the wind pressure center. This center lies on the trailer's body which includes about 80 % of the total external area of the combination model. Once the system is specified, ADAMS proceeds to derive the equations of motion and solve them numerically to provide the vehicle dynamic response. Thus, displacements, velocities, and accelerations of any point or part in the system can be obtained. ADAMS formulations for rigid body are based on those provided by Blundell et al. [21].
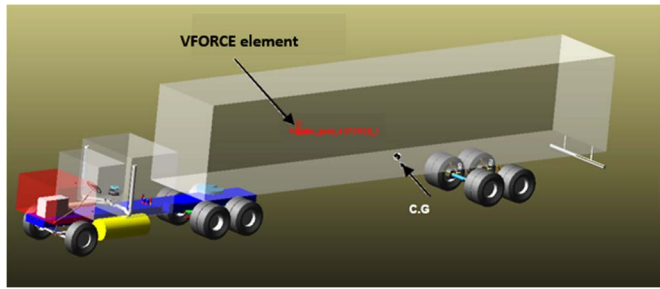

Figure 5 : ADAMS model for a tractor semi-trailer vehicle

A. LTR for the trailer

The Lateral load transfer (LTR) of the trailer unit in nature differs from the lateral load transfer of the tractor unit. However, according to [22], for vehicles with units partly decoupled, load transfer ratio calculations apply better within a single suspension unit. In addition, during path-change maneuver, the trailer unit is more prone to rollover than the tractor due to the rearward amplification tendency of the combination[23]. Hence, in this calculation, the contribution due to the tractor unit is neglected. Therefore, the LTR for the trailer axles (R_i)) is used as a rollover threat index in this analysis as suggested by [5], the ratio is defined as:

$$R_i = \frac{F_{zr} - F_{zl}}{F_{zr} + F_{zl}} \qquad -1 \leq R_i \leq 1 \qquad (7)$$

where F_{zl} and F_{zr} are the vertical loads of the dual tires on the left and right sides respectively, and i represents the front and rear axle of the trailer, see Figure 6. However, under crosswind

condition, the intention is to prevent any wheel from lift-off, thus, the normalized lateral load-transfer index for the entire trailer is,

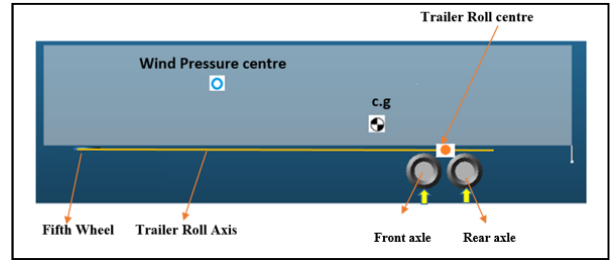$$R_t = \max(R_i) \qquad (8)$$

Figure 6 : Free body diagram of the trailer body

An implementable formula of the LTR can be developed by establishing the balance of vertical forces and roll moments of the sprung mass (m_s) and un-sprung mass (m_{us}) at roll center [4][24]. The roll center is dependent on the kinematic properties of the suspensions and typically located between the height of the center of gravity above the ground [25]. A forward moving vehicle negotiating a turn is depicted in Figure 7. With the assumption of constant roll and pressure centers, the summation and difference of tire forces can be calculated as:
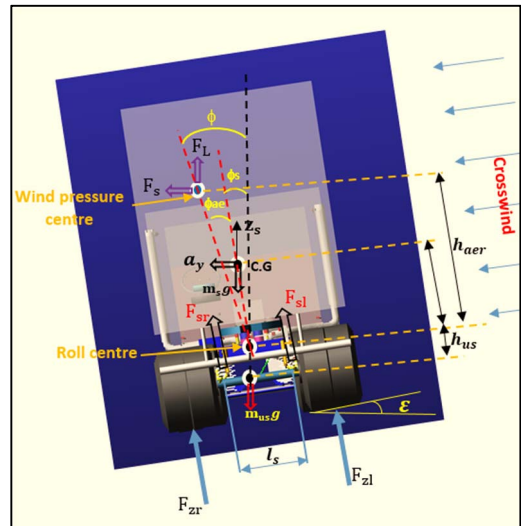

Figure 7 : Free body diagram of the trailer roll model

$$F_{zl} - F_{zr} = \frac{l_s}{l_w}(F_{sl} - F_{sr}) + \frac{2}{l_w}[(F_S \cdot h_{aer} \cdot cos\emptyset) - (F_L \cdot h_{aer} \cdot sin\emptyset) + m_s \cdot g \cdot h_s \cdot sin\emptyset_s + a_y(m_s \cdot h_s \cdot cos\emptyset_s - m_u \cdot h_{us})] \qquad (9)$$

$$F_{zl} + F_{zr} = F_{sl} + F_{sr} - F_L + m \cdot g \qquad (10)$$

Where $\emptyset_s$ and $\emptyset_{ae}$ are roll angles due to suspension and aerodynamic forces respectively. Φ is the total roll angle, other parameters like horizontal and vertical distances between roll center and mass centers are displayed in Figure (7). The suspension forces (F_{sl} , F_{sr}) are given as[26]:

$$F_{sr} = -k\left(z_s - \frac{l_s}{2}sin\emptyset\right) - d\left(\dot{z}_s - \frac{l_s}{2}\dot{\emptyset}\,cos\emptyset\right) \quad (11)$$

$$F_{sl} = -k\left(z_s + \frac{l_s}{2}sin\emptyset\right) - d\left(\dot{z}_s + \frac{l_s}{2}\dot{\emptyset}\,cos\emptyset\right) \quad (12)$$

where k is the suspension stiffness, d is the suspension damping and Z_s is the sprung mass position. Furthermore, as the vehicle is entering a turn of radius R, a centripetal lateral acceleration a_y is generated at vehicle's mass center, and it is given by:

$$a_y = \dot{v}_y + v_x r_t - (h_s\ddot{\phi}_s + h_{aer}\ddot{\phi}_{ae}) = \frac{v_t^2}{R}\cos(\varepsilon) + g\sin(\varepsilon) \quad (13)$$

Where v_x, $\dot{v}_y$ and r_t are vectors of longitudinal, lateral and yaw velocities at vehicle's mass center respectively, and ε is road camber. This acceleration includes the influence of the lateral tire dynamics.

IV. SIMULATION RESULTS

The necessity of a coupled analysis of vehicle aerodynamics and vehicle multi-body dynamics to investigate the vehicle roll stability with a higher accuracy is demonstrated below. For evaluating the LTR indicator of the trailer axles under crosswind in critical scenario, a rollover maneuver was simulated in the ADAMS/Car. The maneuver (Figure 8) involved a constant radius turning, in which the vehicle is exposed to a high level of centripetal acceleration. In this critical scenario, it is assumed that the vehicle negotiates the curve at high constant speed of 25 m/sec and the wind loads acting at the direction of centripetal force. Although, the crosswind is assumed to be perpendicular to the driving direction of the vehicle all the time, the ADAMS solver can consider the variation in wind directions during curved motion.
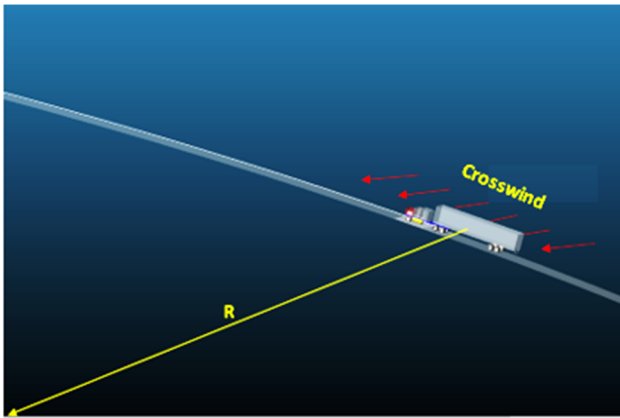

Figure 8: constant radius turning manoeuvre

Figures 9, 10 illustrate the variation of the LTR index of the trailer axles with/without crosswind actions when the trailer moves through a curved road with a typical radius of 260 m. In Figure 9, at the steady-turning maneuver without crosswind effects, the LTR index values for both axles do not change. Under this condition, safety performance of the trailer unit is relatively high, and under the maximum/danger limit of the LTR index, which is at LTR =1. However, under a similar

manoeuvre, but in crosswind conditions, the results in Figure 10 show that the unsteady crosswind actions add transient effects to the steady statw turning manoeuvre. As a result of that, the values of crosswind LTR indices for both axles of the trailer have increased and wheel lift-off condition has been detected for the rear axle of the trailer.
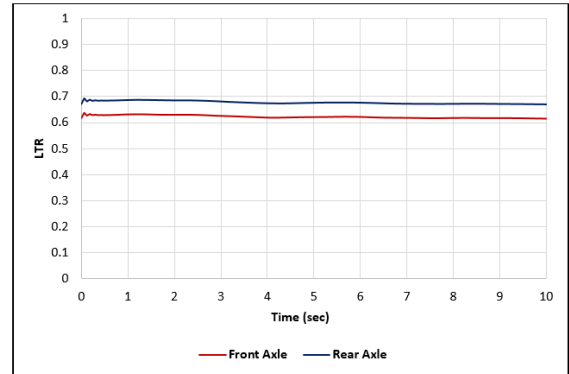

Figure 9: Time dependent of the LTR index of the trailer axles without crosswind effects under constant radius manoeuvre
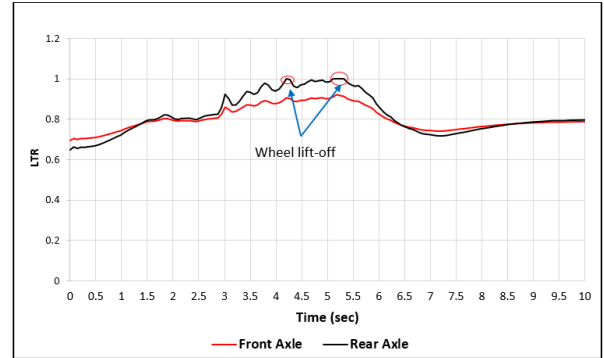

Figure 10: The LTR indicator of the trailer axles with crosswind effects under constant radius manoeuvre
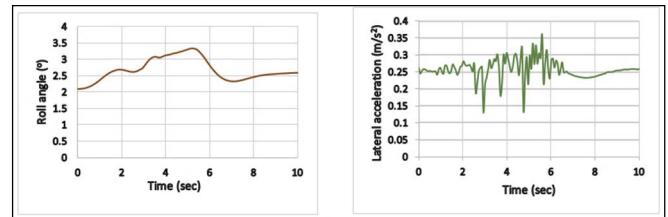

Figure 11 : Variations of roll angle and lateral acceleration of the trailer body during turning manoeuvre with crosswind.

Figure 11 presents time histories of roll angle and lateral acceleration of the trailer body during turning manoeuvre with crosswind effects, which are the input for the LTR indicator. High oscillations in the trailer's body and lateral responses corresponding to the centrifugal and crosswind forces are obserbed. These responses should be considered when developing an active or a passive rollover control systems for a tractor semitrailer vehicle.

CONCLUSION

In this work, an improved method for LTR rollover criteria for a tractor semitrailer vehicle has been developed. Multi-body simulations including unsteady aerodynamic forces obtained by using the LES technique have been performed. Based on this coupled analysis, dynamic responses of the vehicle to fluctuating crosswind conditions have been predicted. All parameters of the LTR index such as body roll angle and lateral acceleration were estimated through a critical turning maneuvers with crosswind actions. The implemented methodology is also useful to analyse the performance of active/passive rollover control systems under strong crosswind environment.

REFERENCES

[1]   T. Chou, and T.-W. Chu, "An improvement in rollover detection of articulated vehicles using the grey system theory," Vehicle System Dynamics, vol. 52, no. 5, pp. 679-703, 2014.

[2]   N. H. T. S. Administration, Initiative to address the mitigation of vehicle rollover, Docket No, NHTSA-2003-14622-1, 2003.

[3]   J. Preston-Thomas, and J. H. Woodrooffe, "FEASIBILITY STUDY OF A ROLLOVER WARNING DEVICE FOR HEAVY TRUCKS," 1990.

[4]   G. Phanomchoeng, and R. Rajamani, "New rollover index for the detection of tripped and untripped rollovers," IEEE Transactions on Industrial Electronics, vol. 60, no. 10, pp. 4726-4736, 2013.

[5]   D. Hyun, and R. Langari, "Modeling to predict rollover threat of tractor-semitrailers," Vehicle System Dynamics, vol. 39, no. 6, pp. 401-414, 2003.

[6]   B. Zhu, Q. Piao, J. Zhao, and L. Guo, "Integrated chassis control for vehicle rollover prevention with neural network time-to-rollover warning metrics," Advances in Mechanical Engineering, vol. 8, no. 2, pp. 1687814016632679, 2016.

[7]   R. Rajamani, D. Piyabongkarn, V. Tsourapas, and J. Y. Lew, "Parameter and state estimation in vehicle roll dynamics," IEEE Transactions on Intelligent Transportation Systems, vol. 12, no. 4, pp. 1558-1567, 2011.

[8]   Y. He, X. Yan, D. Chu, C. Wu, and Z. Chen, "Contribution of wind forces to rollover stability of heavy duty vehicle." In Transportation Information and Safety (ICTIS), 2015 International Conference on (pp. 173-176).

[9]   C. Baker, "High sided articulated road vehicles in strong cross winds," Journal of Wind Engineering and Industrial Aerodynamics, vol. 31, no. 1, pp. 67-85, 1988.

[10]   C. Baker, "The quantification of accident risk for road vehicles in cross winds," Journal of Wind Engineering and Industrial Aerodynamics, vol. 52, pp. 93-107, 1994.

[11]   D. V. Sumantran, and D. G. Sovran, "Vehicle Aerodynamics," Warrendale, PA: Society of Automotive Engineers, 1996. 688, 1996.

[12]   S. Krajnović, P. Ringqvist, K. Nakade, and B. Basara, "Large eddy simulation of the flow around a simplified train moving through a crosswind flow," Journal of Wind Engineering and Industrial Aerodynamics, vol. 110, pp. 86-99, 2012.

[13]   J. García, J. Muñoz-Paniagua, A. Jiménez, E. Migoya, and A. Crespo, "Numerical study of the influence of synthetic turbulent inflow conditions on the aerodynamics of a train," Journal of Fluids and Structures, vol. 56, pp. 134-151, 2015.

[14]   Majda, A. J., & Kramer, P. R. (1999). Simplified models for turbulent diffusion: theory, numerical modelling, and physical phenomena. Physics reports,314(4), 237-574.

[15]   A. Smirnov, S. Shi, and I. Celik, "Random flow generation technique for large eddy simulations and particle-dynamics modeling," Journal of Fluids Engineering, vol. 123, no. 2, pp. 359-371, 2001.

[16]   V. Malviya, N. Gundala, and R. Mishra, "Effect of cross wind on aerodynamic coefficients of ground vehicles," 2009.

[17]   Hucho, W. H. (Ed.). (2013). Aerodynamics of road vehicles: from fluid mechanics to vehicle engineering. Elsevier.

[18]   M. Tsubokura, T. Nakashima, M. Kitayama, Y. Ikawa, D. H. Doh, and T. Kobayashi, "Large eddy simulation on the unsteady aerodynamic response of a road vehicle in transient crosswinds," International Journal of Heat and Fluid Flow, vol. 31, no. 6, pp. 1075-1086, 2010.

[19]   C. Baker, F. Cheli, A. Orellano, N. Paradot, C. Proppe, and D. Rocchi, "Cross-wind effects on road and rail vehicles," Vehicle system dynamics, vol. 47, no. 8, pp. 983-1022, 2009.

[20]   X. Hongguo, P. Tao, L. Hongfei, X. Yan, and R. Xia, "Improved Algorithm of Dynamic Lateral Load Transfer for Tractor-Semitrailer." In Measuring Technology and Mechatronics Automation (ICMTMA), 2011 Third International Conference on (Vol. 2, pp. 374-377). IEEE. pp. 374-377,2011.

[21]   Blundell, M. and D. Harty "The multibody systems approach to vehicle dynamics" Elsevier, 2004.

[22]   F. Boettiger, K. Hunt, and R. Kamnik, "Roll dynamics and lateral load transfer estimation in articulated heavy freight vehicles," Proc. Instn Mech. Engrs, vol. 217, no. Part D, 2003.

[23]   C. Mallikarjunarao, and P. Fancher, Analysis of the directional response characteristics of double tankers, 0148-7191, SAE Technical Paper, 1978.

[24]   Y. Sellami, H. Imine, A. H. El Hadri, and J. Cadiou, Probabilistic detection of rollover risk of heavy vehicles, 0148-7191, SAE Technical Paper, 2008.

[25]   M. G. Balsom, Contribution of Wind Forces to Lateral Acceleration of Tractor Semi-trailer Units: University of New Brunswick (Canada), 2004.

[26]   R. Rajamani, Vehicle dynamics and control: Springer Science & Business Media, 2011.